Eur. Phys. J. D (2015) 69: 21
DOI: 10.1140/epjd/e2014-50551-2

THE EUROPEAN PHYSICAL JOURNAL D

Regular Article

Electron-impact-induced tryptophan molecule fragmentation*

Jelena Tamuliene[1,a], Liudmila G. Romanova[2], Vasyl S. Vukstich[2], Alexander V. Papp[2], and Alexander V. Snegursky[2]

[1] Vilnius University, Institute of Theoretical Physics and Astronomy, 12 A. Goštauto str., 01108 Vilnius, Lithuania
[2] Institute of Electron Physics, National Academy of Sciences of Ukraine, 21 Universitetska str., 88017 Uzhgorod, Ukraine

Received 25 July 2014 / Received in final form 6 October 2014
Published online 16 January 2015 – © EDP Sciences, Società Italiana di Fisica, Springer-Verlag 2015

Abstract. The fragmentation of a gas-phase tryptophan molecule by a low-energy (<70 eV) electron impact was studied both experimentally and theoretically. Various positively charged fragments were observed and analyzed. A special attention was paid to the energy characteristics of the ionic fragment yield. The geometrical parameters of the initial molecule rearrangement were also analyzed. The fragmentation observed was due to either a simple bond cleavage or more complex reactions involving molecular rearrangements.

1 Introduction

An electron-molecule interaction is a fundamental and very important process involved in various fields, e.g. in radiation biology. In this area, low-energy electrons represent the most predominant species formed during a very short time after the deposition of high-energy ionizing quanta into a biological medium [1]. Once produced, they are able to destruct the environing biological molecules such as DNA and proteins, inducing chromosome aberrations, such as cancer, mutations, genetic transformations, etc. [2]. Thus, it is worth to investigate in detail the underlying mechanisms of the above processes by studying the degradation of the biosystem sub-units under the low-energy electron impact.

In our investigation, we studied interactions of low-energy (<70 eV) electrons with tryptophan molecule belonging to the essential amino acids in order to probe the intrinsic properties of the molecule and trace its change(s) under the electron impact. Tryptophan is the metabolic precursor of serotonin, which plays an important role in a sleeping process and is necessary for normal growth in infants and for nitrogen balance in adults. In the standard genetic code, it is encoded as the codon UGG. This molecule, like other amino acids, has several conformers. The L-stereoisomer of tryptophan is used in structural or enzyme proteins, while the D-stereoisomer is occasionally found in naturally produced peptides (for example, in the marine venom peptide contryphan) [3]. The D-isomer of the molecule is not utilized by humans [4], while L-tryptophan is used for coping with insomnia, sleep apnea, depression, anxiety, facial pain, a severe form of a premenstrual syndrome called the premenstrual dysphoric disorder (PMDD), a smoking cessation, grinding teeth while sleeping (bruxism), attention-deficit-hyperactivity disorder, Tourette's syndrome, as well as for improving the athletic performance [5]. Additionally, L-tryptophan is naturally found in animal and plant proteins. However, the studies of the interaction of low-energy particles with tryptophan are scarce: there are some data on the molecule's fragmentation when the negatively charged species are observed (see, e.g. [1]), or on the fragmentation of the radical-cationic tryptophan [6]. To better understand the initial molecular processes taking place during the interaction of radiation with a living system, the results of studying the process of the positively charged fragment formation under the low-energy electron impact using the mass-spectrometric technique are presented here.

A theoretical method was used to predict both possible fragmentation channels and processes that could occur under electron impact, involving the additional ones, such as dehydration and H atom migration.

The theoretical results were compared with the experimentally measured data aiming to check the theoretical predictions made, choose the dominant fragmentation pathways and describe fragmentation processes more correctly. Hence, the goal of our studies was to elucidate the major channels of formation of the most stable tryptophan molecule conformers as the result of the low-energy electron impact.

2 Experimental

The experimental technique used in this work was described in detail in a number of our previous papers (see, e.g. [7–9]). The crossed-beam method with the mass separation of the collision products by means of a magnetic mass-spectrometer was applied. Note, that our apparatus is capable of studying ionic fragments with respect to their mass-to-charge ratio within the 1–720 a.m.u. mass range

* Contribution to the Topical Issue "Elementary Processes with Atoms and Molecules in Isolated and Aggregated States", edited by Friedrich Aumayr, Bratislav Marinkovic, Stefan Matejcik, John Tanis and Kurt H. Becker.

[a] e-mail: Jelena.Tamuliene@tfai.vu.lt

with high sensitivity ($\sim 10^{-16}$ A) and relative mass resolution ($m/\Delta m = 1100$). Below, we shall use the [a.m.u.] units to denote the mass of the fragments produced here, mass is considered as mass-to-charge ratio (m/z). The tryptophan molecular beam was produced by a heated effusion source providing the molecule concentrations of about 10^{10} cm^{-3}. The electron energy scale calibration was carried out on the basis of known ionization thresholds for the Ar atom and N_2 molecule with the accuracy of ± 0.1 eV [7]. The tryptophan molecule mass-spectrum was measured at the 70 eV electron energy, which is typical for mass-spectrometric studies. The appearance energies for the positively charged fragment ions were determined within the 5–30 eV energy range using the fitting technique described in references [7–9]. This technique is based on extracting the appearance energies from the measured near-threshold ion yield curves involving weighted, non-linear least-squares fitting of the initial data using the Marquart-Levenberg algorithm. The estimated absolute accuracy of the appearance energy determination was better than 100 meV and was linear in the energy range under study. The relative theoretical uncertainty being mostly the statistical one (as in the case of experimental measurements as well) did not exceed 5%.

3 Theoretical

Several structures of the tryptophan molecule and its fragments were studied by the Becke's three-parameter hybrid functional [10], applying the non-local correlation provided by Lee et al. (B3LYP) – a representative standard DFT method with the cc-pVTZ basis [11]. The structures of the five molecule conformers and their fragments under study were optimized without any symmetry constraint. The most stable conformer was chosen for the further investigation. In order to model the fragmentation processes, the fragment anions, cations, and fragments with a zero charge both with and without geometry optimization were evaluated to predict the influence of the dissociation energy on the fragmentation processes. The threshold energies were calculated as the difference between the total energy of the investigated conformer of the molecule and the sum of the energies of the fragments predicted, while to evaluate the above influence we studied the following two cases: (i) the single-point energy calculation of the fragments was performed taking into account the geometry of a certain part of the tryptophan molecule (in these cases the energy of fragments formation is not the lowest one); (ii) the structure of the tryptophan fragments was optimized, i.e. the fragments were allowed to reach their equilibrium geometry and the obtained energy (the lowest energy of the fragments) was used to calculate the dissociation energy. The calculated values of the dissociation energy were compared with those of the experimental measurements to select and present results indicating more probable reactions of the newly-formed fragments. The Gaussian program packages were applied here [12,13].

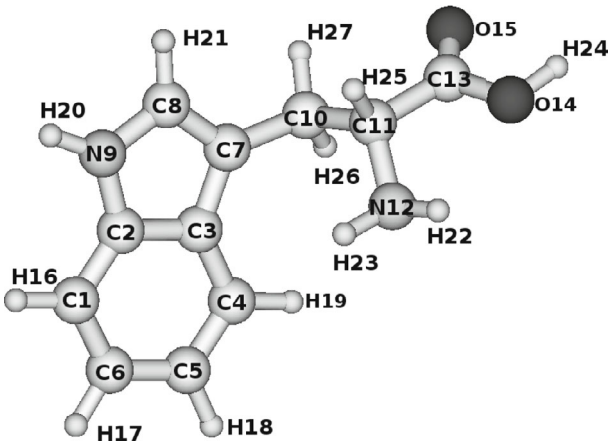

Fig. 1. The tryptophan molecule image and the atom numbers used in this paper. The results of our investigation prove this structure as the most stable one.

4 Results and discussion

The data on the dissociative ionization of amino acids are mostly related to the fact that these biomolecules undergo the fragmentation under the experimental conditions due to the interaction of molecules with the incident electrons producing their dissociative ionization and, in some cases, thermal destruction by heating needed for the converting the microcrystal substance into the gaseous state [14].

4.1 Molecular ion

The tryptophan molecule conformer image and the atom numbers, used in this paper, are presented in Figure 1. The main peculiarity of the tryptophan molecule as compared to other amino acid molecules is the presence of an aromatic indole moiety in the side chain. Indole is the π-excess 10 π-electron aromatic system that includes the lone pair electrons of the nitrogen atom increasing the electron density in the carbon atoms being present both in the pyrrole and benzene parts of the molecule under study [15].

The tryptophan molecule, apart of the indole ring with aromatic electron cloud, comprises two isolated functional groups involving heteroatoms with lone pair electrons, while the carbonyl group comprises π-electrons. The ionization of this molecule with minimal energy consumption could proceed due to the electron loss from the indole π-electron ring, the non-bounding heteroatom n-orbitals and the elimination of the double-bond π-electron.

In general, the incident free electron ionizes the target molecule to form a transitory ion. The parent precursor ion having internal energies below the dissociation energy remains stable [16]. In the case, when the internal energies are higher than the dissociation energy, fragmentation processes start. The ionization tends to cause the weakening of the bonding within the ion as compared to the neutral precursor. A weaker bonding means longer bond lengths in the average indicating a higher tendency towards the bond dissociation. To estimate the changes in

Table 1. The bond length before and after ionization of the tryptophan molecule investigated. The bond length and the bond order values of the indole moiety are underlined.

Bond	Bond length, Å Neutral	Bond length, Å Ionized	Bond order, Neutral	Bond order, Ionized	Bond length difference, Å	Bond order difference
C1-C2	1.394	1.372	1.356	1.475	−0.022	0.119
C1-C6	1.384	1.409	1.538	1.366	0.025	−0.172
C1-H16	1.082	1.081	0.902	0.882	−0.010	−0.020
C2-N9	1.375	1.401	1.015	0.924	0.026	−0.091
C2-C3	1.418	1.417	1.407	1.356	−0.001	−0.051
C3-C4	1.403	1.406	1.366	1.339	0.003	−0.027
C3-C7	1.442	1.419	1.278	1.328	−0.023	0.050
C4-C5	1.383	1.393	1.522	1.433	0.010	−0.089
C4-H19	1.081	1.079	0.870	0.869	−0.002	−0.001
C5-C6	1.405	1.391	1.390	1.493	−0.014	0.103
C5-H18	1.082	1.080	0.910	0.889	−0.002	−0.021
C6-H17	1.082	1.081	0.910	0.889	−0.001	−0.021
C7-C8	1.369	1.420	1.685	1.395	0.051	−0.290
C7-C10	1.500	1.478	0.911	0.957	−0.022	0.046
C8-N9	1.379	1.334	1.038	1.265	−0.045	0.227
C8-H21	1.077	1.078	0.899	0.873	0.001	−0.026
N9-H20	1.003	1.009	0.837	0.806	0.006	−0.031
C10-C11	1.537	1.571	0.905	0.838	0.034	−0.06
C10-H26	1.091	1.091	0.945	0.929	0.00	−0.016
C10-H27	1.089	1.088	0.943	0.918	−0.001	−0.025
C11-N12	1.463	1.437	0.954	0.995	−0.026	0.041
C11-C13	1.523	1.546	0.805	0.807	0.023	0.002
C11-H25	1.103	1.092	0.922	0.937	−0.011	0.015
C13-O14	1.356	1.341	1.018	1.045	−0.015	0.027
C13-O15	1.203	1.200	1.982	1.961	−0.003	−0.021
N12-H22	1.012	1.012	0.864	0.864	0.000	0.000
N12-H23	1.013	1.010	0.864	0.862	−0.003	−0.002
O14-H24	0.968	0.971	0.804	0.789	0.003	−0.015

the tryptophan molecule geometry as the result of ionization, we calculated both the bond lengths and bond orders of the neutral and ionized tryptophan molecules after the geometry optimization. Implementing the Mulliken population analysis data [17], the weakest bonds in the tryptophan molecule were determined. The bond lengths calculated and the bond orders of both the neutral and ionized tryptophan molecules are listed in Table 1.

According to the results obtained for the neutral and ionized tryptophan molecule, the carbon skeleton bonds beyond the indole ring – C10-C11 and C11-C13 are the weakest. Referring to the results presented, it is possible to see that some bonds in the ionized molecule are longer and/or weaker than those in the neutral one. Hence, we may state that the indole part of the tryptophan molecule under the electron impact becomes highly distorted. However, the most abundant ion in the measured spectra is that having the $m = 130$ a.m.u. mass, and this fragment could be formed due to the C_α–C_β (C10-C11) bond cleavage.

Moreover, according to our calculations and including the zero point energy corrections, the first ionization potential of the tryptophan molecule is 7.12 ± 0.02 eV. If the potential energy is minimal and the degree of its excitation is below the energy barrier for the dissociation, the ion may exist for a very long time. The ions, having the internal energy above the dissociation energy level, will dissociate at some point leading to the appearance of the fragment ions in the mass-spectrum under study [18].

The tryptophan molecule mass-spectrum measured at the 70 eV electron energy (see Fig. 2) is generally close to that published in the NIST database [14]. This spectrum is characterized by a high selectivity, since, besides the main channel of the molecular ion dissociation with subsequent production of the fragment with the $m = 130$ a.m.u. mass, the intensities of the most clear peaks corresponding to the ions with the $m = 28$, 77, 103 and 204 a.m.u masses do not exceed 7% of the main peak intensity. It should be noted here that, under the electron impact, a lot of fragments are produced with the peak intensity not exceeding 3% in the mass-spectrum. In general, this mass-spectrum is similar to those measured earlier for this molecule in case of photoionization [19,20] and electron-impact ionization [14]. However, one should note the relatively low-intensity peaks corresponding to the fractional masses $m = 57.5, 64.5, 65.5, 79.5$ a.m.u (the latter being the most intense of them) and a diffuse peak at about $m = 81.5$ a.m.u (a darker-tinted one) indicating

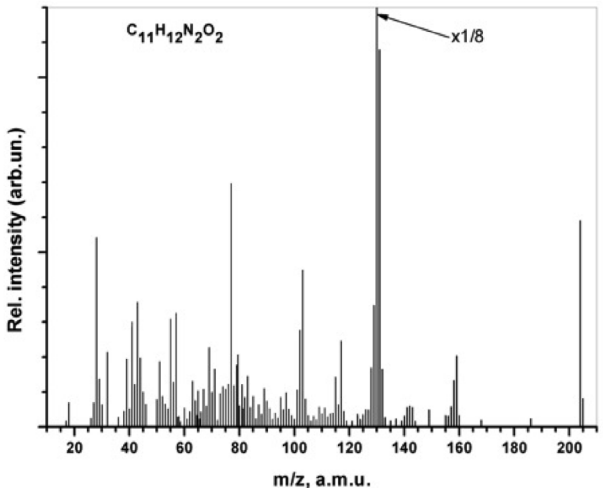

Fig. 2. Tryptophan molecule mass-spectrum.

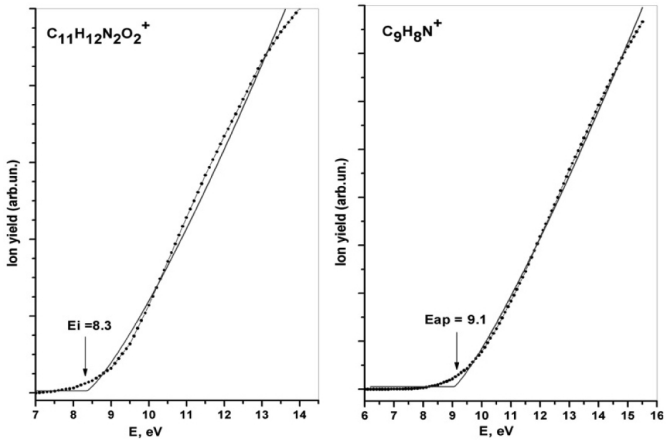

Fig. 3. Yield of the molecular $C_{11}H_{12}N_2O_2^+$ tryptophan ion (a) and its ionic $C_9H_8N^+$ fragment (b) vs. electron energy. Dots – experimental data, solid curves – result of the least-square fitting. E_i – ionization threshold (eV). E_{ap} – ion appearance energy (eV).

the presence of the doubly charged ionic fragments and the ion decaying on its path from the ion source to the detector.

Obviously, the intensities of the aliphatic amine acid molecular ion peaks in the mass-spectra are very low due to the high probability of the decay processes initiated by the cation-radical center localized on the amine group. However, due to the aromatic character of the side chain, tryptophan displays a rather different pattern and the intensity of the parent molecule signal in the mass-spectrum makes the determination of its ionization potential possible.

Using the above algorithm and the experimental initial molecule ionization curve, we determined the ionization threshold for the parent $C_{11}H_{12}N_2O_2$ molecule (m = 204 a.m.u., see Fig. 3a). Its absolute value of 8.3 ± 0.1 eV is slightly lower than the similar value obtained in our investigations for the molecules of some other aliphatic amino acids [8,21–23] and agree with that obtained in the photoelectron spectroscopy experiment: 7.9 (π_1), 8.3 (π_2), 9.8 eV for the first molecular orbitals (MO) of tryptophan [24].

In the case of the aliphatic amino acid molecules, the lowest ionization energy (IE) is mostly related to the NH_2 nitrogen lone pair ionization. However, for aromatic amino acids the lowest IE is obviously related to the ionization of the aromatic ring π molecular orbital that has the ionization potential lower than that for the n-orbital of the nitrogen atom. The vertical ionization energies were calculated in references [25,26] for three conformations of tryptophan, which differ in the relative orientation of the amine and carboxyl heads. It is known that the conformation can have a dramatic effect on the order of the ionized MOs and, thus, on the IEs. So, for three tryptophan conformers, the vertical IE calculated using the outer-valence-Green's-functions (OVGF) method for the neutral molecule geometry lies within the 7.07–7.34 eV interval. For all the conformers the order of the first three MOs is the same and there are the $\pi 1$, $\pi 2$ and $\pi 3$ orbitals of the indole unity. The difference in the MO character is caused by a spatial orientation of the functional groups. The first ionization threshold value for the tryptophan molecule calculated using different methods is 7.22–7.88 eV [26]. According to our calculations, the ionization energy calculated as the difference in the energies between the tryptophan cation and the neutral molecule is 7.12 eV, so this value coincides excellently with the data of reference [26].

4.2 High intensity fragments

Structurally, tryptophan, as the aromatic amino acid, could be presented as the indole-3-alanine or the 3-methyleneindole bound at the C_α position to a residue of a simple amino acid (glycine). The ion fragment $C_9H_8N^+$ corresponding to the dominant mass-spectrum peak, independent of the ionization way [14,19,20], is produced due to the C_α–C_β (C10-C11) bond rupture in the initial molecule. The fraction of the complementary ion with the mass of m = 74 a.m.u. (i.e. $C_2H_4NO_2^+$) is about 1% of the main peak. Thus, the tryptophan molecule ionization proceeds mainly due to electron elimination by the methyleneindole group of the molecule at which the positive charge is predominantly localized:

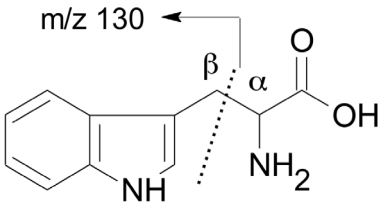

The bond break between the indole group and $–CH_2$-$C(NH_2)$-COOH occurs as well. However, this dissociation channel is not efficient: the intensity of the $m = 117$ a.m.u. peak corresponding to the indole molecule ion does not exceed 4% of the main peak in the mass-spectrum. The dominant C10-C11 bond rupture as compared to the C4-C10

Table 2. Calculated threshold energies (in eV) for the C_9H_8N and $C_2H_4NO_2$ fragments formed.

C_9H_8N ($m = 130$ a.m.u.) fragment charge	$C_2H_4NO_2$ ($m = 74$ a.m.u.) fragment charge	Calculated threshold energy
1	−1	7.59
1	0	8.07
−1	1	9.08
0	1	9.12

Table 3. Calculated threshold energies (in eV) for the $C_2H_3NO_2$ and C_9H_8N + H fragments formed when the O-H bond is broken.

$C_2H_3NO_2$ ($m = 73$ a.m.u.) fragment charge	(C_9H_8N + H) ($m = 131$ a.m.u.) fragment charge	Calculated threshold energy
−1	1	7.36
0	1	8.58

one is, in our opinion, due to the difference in the IEs of the fragments produced. Thus, E_i of the 3-methylindole was determined in reference [27] as 7.52 eV, while that for indole is 7.76 eV [28]. From the thermodynamic point of view, in the case of the molecular ion dissociation, the charge is located on the fragment with lower ionization potential and the fragmentation most probably proceeds via the nearest to the charge localization places simple bonds. At the electron energies slightly exceeding the tryptophan molecule ionization potential E_i the probability of the C10-C11 bond dissociation is very high. At higher energies, when the electron energy is sufficient to ionize deeper molecular orbitals, first of all those of the nitrogen and oxygen lone pairs, it will result in a dissociation of the neighboring bonds thus producing, more fragmentation channels. However, as it is seen from our mass-spectrum data, the signal intensity of fragments resulting from such channels is insignificant because the aromatic group stabilizes the positive charge and reduces the fragmentation.

As mentioned earlier, the main peak in the tryptophan mass spectrum is due to the $C_9H_8N^+$ ion produced at a simple cleavage of the C_α–C_β (C10-C11) bond of the initial molecule. The charge is mainly localized on the fragment comprising the aromatic indole ring. The calculated binding energy per atom for the $C_9H_8N^+$ fragment is equal to 5.44 eV and is higher than that of the complementary ion with the $m = 74$ a.m.u. mass (3.92 eV). These results indicate a high stability of the $m = 130$ a.m.u. fragment and a larger possibility of its formation. Hence, the peak at the $m = 74$ a.m.u. mass is not intense in the tryptophan mass spectrum. The inclusion of any possible cases of charge distribution at this bond dissociation results in production of the C_9H_8N and $C_2H_4NO_2$ fragments according to the following pathways:

$$C_{11}H_{12}N_2O_2 + e \rightarrow \begin{cases} C_9H_8N^+ + C_2H_4NO_2^- + e & (1) \\ C_9H_8N^+ + C_2H_4NO_2^0 + 2e & (2) \\ C_9H_8N^- + C_2H_4NO_2^+ + e & (3) \\ C_9H_8N^0 + C_2H_4NO_2^+ + 2e. & (4) \end{cases}$$

The lower stability of the $C_2H_4NO_2^+$ ion as compared to that of the $C_9H_8N^+$ fragment and its higher threshold energy confirm the experimental results, i.e. the probability of the formation of a positively charged glycyl fragment is lower than that of the C_9H_8N one. These results coincide with the observations of MacLennan et al. [29] that indicate the C_α–C_β (C10-C11) bond cleavage with the elimination of the cationic side-chain fragment, $C_9H_8N^+$ as a low-energy process, while the production of $C_2H_4NO_2^+$ is shown as a high-energy process.

According to the energy dependence of the $C_9H_8N^+$ ion ($m = 130$ a.m.u.) formed from the parent tryptophan molecule (see Fig. 3b), we determined its appearance potential as 9.1 ± 0.1 eV and this value slightly (by 0.93 eV) exceeds the obtained theoretical one for pathway (2).

In the tryptophan mass-spectrum, the peak with the $m = 131$ a.m.u mass is the second by its intensity, and the ratio of intensities of the ion peaks with the $m = 130$ and $m = 131$ a.m.u. masses at the 70 eV electron ionization energy shows, in our opinion, that the ion peak at $m = 131$ a.m.u. is the first isotope peak. It should be noted that the intensity of this peak at photoionization by the noble gas resonance radiation at the 21.2 eV energy, quoted in reference [20] (17.8% of the main peak intensity), exceeds considerably the calculated value of the first isotope peak intensity (10.3%). So we analyzed two possibilities of the $m = 131$ a.m.u. fragment formation due to the intramolecular hydrogen transfer, i.e. the cleavage of the C_α–C_β bond is accompanied by the hydrogen atom transfer from the O-H or N12-H23 bond, whereas the H atom is joined to the C_9H_8N fragment. The above possibilities are chosen according to the results of the studies on the bond orders and bond lengths of the ionized and neutral molecules, i.e. the O-H bonds become the weakest ones in the ionized molecule, while the N12-H23 bond is one of the nearest to the weak bond because of the C_9H_8N fragment. The threshold energy calculated indicates the pathway of formation of the $m = 131$ a.m.u. fragment due to the intramolecular hydrogen transfer as very possible (see Tabs. 3 and 4).

Probably, at low ionizing radiation energy (21.2 eV), the intramolecular hydrogen transfer reaction for tryptophan is significant, and the probability of the hydrogen atom migration from the hydroxyl group to the indole ring is larger than that for the amino group. However,

Table 4. Calculated threshold energies (in eV) for the $C_2H_3NO_2$ and C_9H_8N fragments formed when the N-H bond is broken.

$C_2H_3NO_2$ ($m = 74$ a.m.u.) fragment charge	C_9H_8N ($m = 130$ a.m.u.) fragment charge	Calculated threshold energy
−1	1	12.13
0	1	12.47

Table 5. Calculated threshold energies (in eV) for the $C_8H_7^+$ fragment formed.

C_8H_7 ($m = 103$ a.m.u.) fragment charge	($CH_2N + C_2H_3NO_2$) fragment charge	Calculated threshold energy
1	−1	8.65
1	0	12.79

Table 6. Calculated threshold energies (in eV) for the $C_7H_5N^+$ fragment formed.

C_7H_5N ($m = 103$ a.m.u.) fragment charge	($H + C_4H_6NO_2$) fragment charge	Calculated threshold energy
1	−1	14.43
1	0	12.02
1	1	20.54

at the 70 eV energy the peak at $m = 131$ a.m.u. has the isotope character and it is indirectly confirmed by the peak at $m = 132$ a.m.u. with the intensity of about 10% of that of the peak at $m = 131$ a.m.u. corresponding to the calculated value for the second isotope peak $^{13}C_2C_7H_8N^+$.

In the tryptophan mass spectrum, the peaks with the $m = 103$ and 77 a.m.u. masses demonstrate significant intensities and could be produced due to the initial molecule dissociation and result from the secondary fragmentation of the 3-methyleneindole ($C_9H_8N^+$, $m = 130$ a.m.u.) molecule. The main channels of the dissociative ionization of the above molecule lead to the production of the ions with the $m = 103$ a.m.u. (10%) and $m = 77$ a.m.u. (14%) masses [30].

The mass $m = 103$ a.m.u. may correspond to the two isobaric ions with the gross-formula $C_8H_7^+$ and $C_7H_5N^+$. The fragment C_8H_7 with the vinyl-benzene structure is formed when the cleavage of the C_α–C_β bond is accompanied by a hydrogen atom transfer from the COOH group to the indole ring and the formation of the CH_2N ($m = 28$ a.m.u.) fragment from the N9, C8 and H20, H21 atoms. The N9-C2 and C8-C7 bond elongation and the bond order value decrease in the ionized molecule as compared to those of the neutral one indicate that the destruction of the indole ring of the tryptophan molecule is possible (Tab. 1). The minimum energy-consuming pathway (see Tab. 5) of the fragment C_8H_7 appearance is as follows:

$$\begin{aligned} C_{11}H_{12}N_2O_2 + e &\rightarrow (C_8H_6 + H)^+ \\ &+ (CH_2N + C_2H_3NO_2)^- + e \rightarrow C_8H_7^+ \\ &+ (CH_2N + C_2H_3NO_2)^- + e. \end{aligned} \quad (5)$$

We calculated the threshold energy for the other isobaric fragment with the $m = 103$ a.m.u. mass having the isocyanobenzene structure and produced via the following pathways:

$$C_{11}H_{12}N_2O_2 + e \rightarrow \begin{cases} C_7H_5N^+ + C_4H_7NO_2^- + e & (6) \\ C_7H_5N^+ + C_4H_7NO_2^0 + 2e & (7) \\ C_7H_5N^- + C_4H_7NO_2^+ + e & (8) \\ C_7H_5N^0 + C_4H_7NO_2^+ + 2e. & (9) \end{cases}$$

Several structural isomers of this ion with different initial molecule bonds ruptured were investigated. Our calculations show that the minimal energy consumption is required to form the fragment with the isocyanobenzene structure. The threshold energy calculated for the C_7H_5N fragment with this structure is presented in Table 6 and indicates pathway (7) as the most probable one.

The comparison of the threshold energies calculated by us for the isobaric ions with the $m = 103$ a.m.u. mass allows leads to the statement that in the near-threshold incident electron energy region the C_8H_7 fragment with the vinyl-benzene structure is produced. Above 12–15 eV, the dissociation of the C7-C8 and C7-C3 bonds and production of the $C_7H_5N^+$ ion become possible.

The ion peak with the $m = 77$ a.m.u. mass could correspond to the two isobaric fragments, i.e. the C_6H_5 and C_5H_3N ones. The formation of the latter fragment, taking into account the minimal number of the structural changes, is possible at the rupture of the three skeleton bonds, when two of which have the bond order more than 1. On the other hand, the possibility of rupturing the bonds with the order of more than 1 is very little. Thus, we assume that the C_5H_3N fragment could be formed due to the indole ring destruction and the cleavage of the C_α–C_β bond (the calculated threshold energies for this ion are presented in Tab. 7).

The threshold energy value for this fragment confirms both the complicated way of its production and

Table 7. Calculated threshold energies (in eV) for the $C_5H_3N^+$ fragment formed.

C_5H_3N ($m = 77$ a.m.u.) fragment charge	C_4H_4+ H + $C_2H_4NO_2$ fragment charge	Calculated threshold energy
1	−1	20.15
1	0	20.04

Table 8. Calculated threshold energies (in eV) for the $C_6H_5^+$ fragment formed.

C_6H_5 ($m = 77$ a.m.u.) fragment charge	$C_5H_7N_2O_2$ ($m = 127$ a.m.u.) fragment charge	Calculated threshold energy
1	−1	14.07
1	0	14.65

Table 9. Calculated threshold energies (eV) for the C_8H_7N and $C_3H_5NO_2$ fragments.

C_8H_7N ($m = 117$ a.m.u.) fragment charge	$C_3H_5NO_2$ ($m = 87$ a.m.u.) fragment charge	Calculated threshold energy
−1	1	9.82
0	1	8.62
1	−1	8.40

Table 10. Calculated threshold energies (eV) for the C_8H_5N and $C_3H_7NO_2$ fragments.

$C_3H_7NO_2$ ($m = 89$ a.m.u.) fragment charge	C_8H_5N ($m = 115$ a.m.u.) fragment charge	Calculated threshold energy
−1	1	14.40
0	1	13.31
1	−1	11.74
1	0	13.83

the stepwise character of this process, i.e. the cleavage of the C_α–C_β bond is accompanied by the vinyl acetylene molecule elimination.

The $C_6H_5^+$ ion is obviously the phenyl-radical that can be formed due to the dissociation of the C2-N9 and C3-C7 bonds of the tryptophan molecule followed by the hydrogen atom migration. The calculated threshold energies for this ion formed with minimal structural changes are presented in Table 8.

Our calculations of the threshold energies for the isobaric fragments with $m = 77$ a.m.u. show that the $C_6H_5^+$ ion is most likely to be produced below 20 eV, while above this energy – the C_5H_3N fragment could be formed.

4.3 Low intensity fragments

In the case of one hydrogen atom migration from the aliphatic chain to the indole moiety in the initial tryptophan molecule, the C7-C10 bond rupture leads to the following complementary ions with the indole (C_8H_7N) and alanine ($C_3H_5NO_2$) structure formation with the ratio (5:1):

$$C_{11}H_{12}N_2O_2 + e \rightarrow \begin{cases} C_8H_7N^- + C_3H_5NO_2^+ + e & (10) \\ C_8H_7N^0 + C_3H_5NO_2^+ + 2e & (11) \\ C_8H_7N^+ + C_3H_5NO_2^- + e & (12) \\ C_8H_7N^+ + C_3H_5NO_2^0 + 2e. & (13) \end{cases}$$

The calculated threshold energies for these fragments are shown in Table 9. The calculated threshold energy values for the indole ion are somewhat lower than those for the ion with the $C_3H_5NO_2$ structure of dehydroalanine formed when the C7-C10 and C11-H25 bonds are broken.

Moreover, on the basis of our calculations, the threshold energy value for the $C_8H_7N^+$ ion according to pathway (13) is 0.17 eV larger than the electron binding energy for the π_1-orbital of the indole group from the photoemission valence spectrum of tryptophan [20], i.e. the dissociation of the C7-C10 bond of the tryptophan molecule is possible at the high-order molecular orbital ionization. In this case, the dominant stabilization of the charge by the indole ring, as compared to the aliphatic amino acid residue, agrees fairly well with the ionization energies for the above tryptophan molecule components.

In the case of the hydrogen atom transfer in the transient ion from the indole ring to the aliphatic group, the dissociation of the C7-C10 group leads to the appearance of the complementary $C_3H_7NO_2$ and C_8H_5N fragments (see their appearance energies in Tab. 10). The ratio of the ion peak intensities corresponding to the fragments with 115−117 a.m.u. masses indicates a higher stability of the positively charged indole ion at the two hydrogen atoms loss as compared to the case when only one hydrogen atom is lost.

In the parent molecule spectrum area of 25–30 a.m.u., the most intense peak is of the ion with the $m = 28$ a.m.u. mass. Indeed, this fragment may be CH_2N and/or CO as it

Table 11. Calculated threshold energies (in eV) for the CH_2N^+ and ($COOH + C_9H_8N$) fragments.

CH_2N ($m = 28$ a.m.u.) fragment charge	($COOH + C_9H_8$) fragment charge	Calculated threshold energy
1	−1	9.64
1	0	12.31
1	1	16.62

Table 12. Calculated threshold energies (in eV) for the CH_2N^+ and $C_{10}H_{10}NO_2$ fragments formed.

CH_2N ($m = 28$ a.m.u.) fragment charge	$C_{10}H_{10}NO_2$ ($m = 176$ a.m.u.) fragment charge	Calculated threshold energy
1	−1	12.82
1	0	15.46

can be observed in other mass spectra of amine acids such as alanine, methionine, glycine [21,25,31]. The formation of the $m = 28$ a.m.u. fragment and the comparison of the stability of the positively charged CH_2N^+ and CO^+ ions indicate the CH_2N^+cation is more probable than the CO^+ one. Moreover, the comparison of the bond length and the order of the neutral and ionized tryptophan molecule proves that the CH_2N fragment formation is more probable than that of the CO one. It should be mentioned that we calculated the threshold energy of the cation formation by two possible pathways:

$$C_{11}H_{12}N_2O_2 + e \rightarrow CH_2N^+ + (C_{10}H_{10}NO_2)^{-/0} + ne \quad (14)$$

$$C_{11}H_{12}N_2O_2 + e \rightarrow CH_2N^+ + (COOH{+}C_9H_8N)^{-/0} + ne, \quad (15)$$

where $n = 1$ or 2 only.

The calculated threshold energies for the $m = 28$ a.m.u. fragment by two possible pathways (14) and (15) are presented in Tables 11 and 12.

The analysis of the threshold energy of the $m = 28$ a.m.u. fragment indicates that the channel with C11-N12H_2 elimination is energetically preferable, although, at the energies above 15.5 eV, the destruction of the indole ring due to electron impact, followed by the CH_2N^+ ion possible formation.

On the other hand, it is necessary to mention that, according to pathway (5), the CH_2N fragment ($m = 28$ a.m.u.) is also produced. There is a very slight possibility that the CH_2N fragment could be charged positively in the $(CH_2N + C_2H_3NO_2)^-$ compound because $C_2H_3NO_2^{-2}$ could be formed in this case. Besides, CH_2N^+ could be formed during the secondary fragmentation of the $m = 130$ a.m.u. fragment ($C_9H_8N^+$). In this case, the minimal calculated energy required for this secondary dissociation is 5.84 eV, and the total energy required for this two-stage process is 13.43–13.91 eV, depending on the fragment charge distribution.

4.4 Doubly charged fragments

In the tryptophan molecule mass-spectrum, the peaks with the fractional masses corresponding to the doubly charged ions are revealed. The most intense peak corresponds to the $C_{10}H_{11}N_2^{2+}$ ion and results from the carboxyl group detachment from the parent molecule. The intensity of this doubly charged ion is approximately the same as that for the relevant singly charged ion. At the protonated tryptophan ionization under the single-collision conditions [32], the yield curve for the ion with the $m = 159$ a.m.u. mass has its maximum what testifies to the predisposition of this ion to the secondary dissociation. Probably, the detachment of the carboxyl group leads to the formation of a conjugated bond system in the aliphatic part of the molecule, favoring the charge stabilization by this fragment.

The low intensity peaks with the $m = 57.5$, 64.5 and 65.5 a.m.u. masses correspond to the $C_8H_5N^{2+}$, $C_9H_7N^{2+}$ and $C_9H_9N^{2+}$ ions, respectively, and demonstrate the indole ring ability to keep stability when detaching the different number of the hydrogen atoms with the simultaneous elimination of two electrons.

The $C_8H_5N^{2+}$ fragment could be formed from the neutral tryptophan due to the C7-C10 bond destruction and the simultaneous H atom migration from the $C_8H_6N^+$ fragment. We calculated the threshold energy of this fragment for both cases. The comparison of the threshold energies obtained proves the formation of $C_8H_5N^{2+}$ according to the following pathway, requiring the minimal energy:

$$C_8H_6N^+ - e \rightarrow C_8H_5N^{2+} + H^0. \quad (16)$$

Referring to the results of the threshold energy calculation, we predict the two possible ways of $C_9H_7N^{2+}$ formation according to the following schemes:

$$C_{11}H_{12}N_2O_2 + e \rightarrow C_9H_7N^{2+} + C_2H_5NO_2^0 + 3e, \quad (17)$$

where the C10-C11 bond destruction is accompanied by the H26 atom migration producing a stable glycine molecule and

$$\begin{array}{l} C_{11}H_{12}N_2O_2 + e \rightarrow C_9H_8N^+ + C_2H_4NO_2^- + e \\ \qquad\qquad\qquad\qquad\quad \searrow \\ \qquad\qquad\qquad\qquad\quad C_9H_7N^{2+} + H^0 + e \end{array} \quad (18)$$

with the hydrogen atom detachment from the doubly charged fragment as a result of the secondary dissociation.

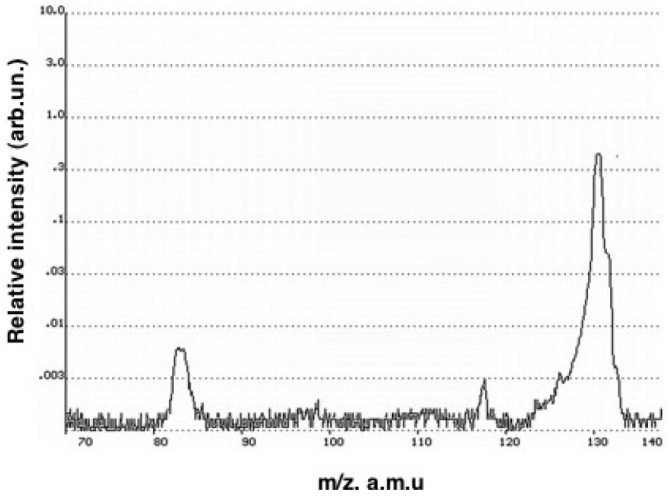

Fig. 4. The area of the tryptophan molecule mass-spectrum at the 18 eV electron energy.

The calculated threshold energy for the $C_9H_7N^{2+}$ fragment is equal to 22.99 eV in the case of (17), while that in the case of (18) is equal to not less than 25.91 eV, i.e. 7.59 eV and 18.32 eV energies are required to produce $C_9H_8N^+$ and $C_9H_7N^{2+}$, respectively. Hence, pathway (17) is more energetically favorable to producing the doubly charged $C_9H_7N^{2+}$ ion.

The $C_9H_9N^{2+}$ ion in this case could be produced as follows:

$$C_{11}H_{12}N_2O_2 + e \rightarrow C_9H_9N^{2+} + (C_2H_3NO_2)^{-/0} + ne \quad (n = 2, 3). \tag{19}$$

The iminoacetic acid is formed as the complementary fragment, and the appearance energy for the $C_9H_9N^{2+}$ doubly charged ion is approximately 21.59 eV and 21.32 eV for the negatively charged one and the neutral iminoacetic acid, respectively.

4.5 Metastable decay

Regarding the peak at about $m = 81.5$ a.m.u., its presence at the ionizing electron energy 18 eV (see Fig. 4) shows that this peak does not correspond to the doubly charged ion, while the fuzzy shape of this peak indicates the presence of a metastable ion with the lifetime less than 10^{-6} s so it decays on its path from the ion source to detector. The estimation of the masses of the initial (m_1) and resulting (m_2) ions using formula $m^* = m_2^2/m_1$, where m^* is the diffuse peak mass, shows that the peak at $m \sim 81.5$ a.m.u. corresponds to the decay of the ion with the $m = 130$ a.m.u. mass, and the production of the ion with the $m = 103$ a.m.u. mass.

Since our mass-spectrum reveals the peaks with the $m = 103$ and 130 a.m.u. masses and the diffuse peak with the $m \sim 81.5$ a.m.u. mass, this means that at least a part of the $C_8H_7^+$ ions is produced directly from the $C_9H_8N^+$ ion. Thus, at the internal energy excess, the methyleneindole ion decays producing the $C_8H_7^+$ ion.

5 Conclusions

Both experimental and theoretical studies on the fragmentation of the tryptophan molecule under electron impact were carried out. The analysis of the tryptophan molecule mass spectrum accompanied by theoretical calculations allowed the main dissociation mechanisms of the above molecule under the low-energy electron impact to be determined. Most of the peaks in the experimental mass spectrum were identified. The absolute values of the ionization energy of the parent $C_{11}H_{12}N_2O_2$ molecule and the appearance energies for its most prominent fragments were determined.

The main fragment under the tryptophan electron-impact dissociation is produced at a simple cleavage of the C_α–C_β (C10-C11) bond of the initial molecule. The C10-C11 bond dissociation is the most probable when the electron energies are slightly exceeding the tryptophan molecule ionization potential. When the electron energy is sufficient to ionize the deeper molecular orbitals, first of all, the lone pair ones of nitrogen and oxygen, dissociation of the O and N atom neighboring bonds takes place, and, as consequence, more fragmentation channels occur. However, the number of such dissociation channels is not significant, because the aromatic group stabilizes the positive charge and reduces the fragmentation.

We seem to be the first to observe the low-intensity peaks in the tryptophan mass spectrum with the $m = 57.5$, 64.5 and 65.5 a.m.u. masses corresponding to the $C_8H_5N^{2+}$, $C_9H_7N^{2+}$ and $C_9H_9N^{2+}$ doubly charged ion production. The indole ring demonstrated stability when the different numbers of the hydrogen atoms were detached together with the simultaneous elimination of two electrons. We also observed the diffuse peak at about $m = 81.5$ a.m.u. that corresponds to the decay of the ion with the $m = 130$ a.m.u. mass and simultaneously produces the $m = 103$ a.m.u. mass ion. Thus, the peak with the $m = 103$ mass having significant intensity could be produced not only due to the initial molecule dissociation but may also result from the secondary fragmentation of the 3-methyleneindole part of the parent molecule.

The authors would like to thank Prof. M. Cegla from Jagellonian University (Krakow, Poland) and our colleague V. Patasiene for their assistance and fruitful discussions. Special thanks go to InSpire and NGI.LT projects for the resources and technical support provided.

References

1. H. Abdoul-Carime, S. Gohlke, E. Illenberger, Chem. Phys. Lett. **402**, 497 (2005)
2. A.F. Fuciarelli, J.D. Zimbrick, *Radiation Damage in DNA: Structure/Function Relationship at Early Times* (Battelle Press, Columbus, 1995)
3. P.K. Pallaghy, A.P. Melnikova, E.C. Jimenez, B.M. Olivera, R.S. Norton, Biochemistry **38**, 11553 (1999)

4. L.V. Hankes, R.R. Brown, J. Leklem, M. Schmaeler, J. Jesseph, J. Invest. Dermatol. **58**, 85 (1972)
5. J. Thomson, H. Rankin, G.W. Ashcroft, C.M. Yates, J.K. McQueen, S.W. Cummings, Psychol. Med. **12**, 741 (1982)
6. H. Kang, C. Dedonder-Lardeux, C. Jouvet, S. Martrenchard, G. Grégoire, C. Desfrançois, J.-P. Schermann, M. Barat, J.A. Fayeton, Phys. Chem. Chem. Phys. **6**, 2628 (2004)
7. V.S. Vukstich, A.I. Imre, A.V. Snegursky, Tech. Phys. Lett. **15**, 1071 (2009)
8. V.S. Vukstich, A.I. Imre, L.G. Romanova, A.V. Snegursky, J. Phys. B **43**, 185208 (2010)
9. V.S. Vukstich, A.I. Imre, A.V. Snegursky, Instrum. Exp. Tech. **54**, 66 (2011)
10. A.D. Becke, J. Chem. Phys. **98**, 5648 (1993)
11. R.A. Kendall, T.H. Dunning Jr., R.J. Harrison, J. Chem. Phys. **96**, 6796 (1992)
12. J.T. Bursey, M.M. Bursey, D.G.I. Kingston, Chem. Rev. **73**, 231 (1973)
13. Gaussian 03, Revision C.02 (Gaussian, Inc., Wallingford CT, 2004)
14. National Institute of Standards (NIST), Standard Reference Database: Chemistry Webbook, http://webbook.nist.gov
15. O.V. Kharitonova, in *Methods and Technology of Production of Organic Compounds Used in Materials for Information Registration* (MITHT Publishers, Moscow, 2004), Part I
16. A. Kraj, D.M. Desiderio, N.M. Nibbering, in *Mass Spectrometry: Instrumentation, Interpretation, and Applications*, edited by R. Ekman, J. Silberring, A. Westman-Brinkmalm (John Wiley & Sons, 2009)
17. R.S. Mulliken, J. Chem. Phys. **23**, 1833 (1955)
18. H. Jurgen, *Gross Mass Spectroscopy. A Textbook*, 2nd edn. (Springer-Verlag, Berlin-Heidelberg, 2011)
19. F.O. Talbot, T. Tabarin, R. Antoine, M. Broyer, P. Dugourd, J. Chem. Phys. **122**, 074310 (2005)
20. O. Plekan, V. Feyer, R. Richter, M. Coreno, K.C. Prince, Mol. Phys. **106**, 1143 (2008)
21. J. Tamuliene, L.G. Romanova, V.S. Vukstich, A.V. Snegursky, Chem. Phys. **404**, 74 (2012)
22. V.S. Vukstich, L.G. Romanova, A.V. Snegursky, Tech. Phys. Lett. **38**, 347 (2012)
23. J. Tamuliene, L.G. Romanova, V.S. Vukstich, A.V. Snegursky, Chem. Phys. **404**, 36 (2012)
24. P.H. Cannington, N.S. Ham, J. Electron Spectrosc. Relat. Phenom. **32**, 139 (1983)
25. V. Lepere, B. Lucas, M. Barat, J.A. Fayeton, V.J. Picard, C. Jouvet, P. Carcabal, I. Nielsen, C. Dedonder-Lardeux, G. Gregoire, A. Fujii, J. Chem. Phys. **127**, 134313 (2007)
26. D. Dehareng, G. Dive, Int. J. Mol. Sci. **5**, 301 (2004)
27. D. Q. Liu, M. Sun, ISRN Spectrosc. **2012**, 973649 (2012)
28. J. Hager, M. Ivanco, M.A. Smith, S.C. Wallace, Chem. Phys. **105**, 397 (1986)
29. M.S. MacLennan, K.N. Sutherland, G. Orlova, J. Mol. Struct. (Theochem) **822**, 21 (2007)
30. V.S. Vukstich, L.G. Romanova, I.G. Megela, A.V. Snegursky, Tech. Phys. Let. **40**, 263 (2014)
31. J. Tamuliene, L.G. Romanova, V.S. Vukstich, A.V. Snegursky, Lith. J. Phys. **53**, 195 (2013)
32. H. El Aribi, G. Orlova, A.C. Hopkinson, K.W.M. Siu, J. Phys. Chem. A **108**, 3844 (2004)